Water Sorption Thermodynamics in Polymer Matrices

Pellegrino Musto, Michele Galizia, Giuseppe Scherillo and Giuseppe Mensitieri

Abstract Water sorption is a key issue in assessing the durability of polymer matrix composites. In fact absorbed water can adversely affect mechanical properties of the matrix and fibre-matrix interface integrity. In this contribution the general issue of water sorption thermodynamics in polymers is addressed from the experimental and theoretical point of view. The case of both rubbery and glassy polymers is considered modelling thermodynamics of water-polymer systems using lattice fluid theories accounting also for the occurrence of possible self- and cross-hydrogen bonding interactions. Outcomes of theoretical analyses are compared to experimental results obtained by vibrational spectroscopy and gravimetric measurements.

1 Introduction

Hygrothermal aging of polymer matrices is related to sorption of water molecules within the material [1] which promotes plasticization of the polymer depressing its glass transition temperature, T_g, [1] and, eventually, hydrolytic degradation. The amount of water absorbed at equilibrium heavily depends upon the chemical

P. Musto
Institute of Chemistry and Technology of Polymers, National Research Council of Italy, Via Campi Flegrei 34, Olivetti Buildings 80078 Pozzuoli, NA, Italy
e-mail: pellegrino.musto@ictp.cnr.it

M. Galizia · G. Scherillo · G. Mensitieri (✉)
Department of Chemical, Materials and Production Engineering, University of Naples Federico II, P.le Tecchio 80 80125 Naples, Italy
e-mail: mensitie@unina.it

M. Galizia
e-mail: michele-galizia@unina.it

G. Scherillo
e-mail: gscheril@unina.it

P. Davies and Y. D. S. Rajapakse (eds.), *Durability of Composites in a Marine Environment*, Solid Mechanics and Its Applications 208,
DOI: 10.1007/978-94-007-7417-9_2,

structure and morphology of the polymer. The understanding of this phenomenon is a crucial task for the assessment of long term durability of a polymer based composite material and for the understanding of possible effects like matrix cracking, microvoid generation, outer-ply delamination or surface blistering. In Fig. 1 is reported a schematic illustration of water transport, sorption and interaction mechanisms occurring in polymer matrix composites along with possible induced damages.

In view of these premises, understanding and modelling sorption thermodynamics of water in rubbery and glassy polymers is of great importance from both fundamental and technological standpoints. Synergic combination of theoretical and experimental approaches allows a quantitative treatment of water sorption thermodynamics accounting also for water-polymer specific interactions. In fact, the use of infrared vibrational spectroscopy combined with gravimetric measurements can lead to a quantitative experimental evaluation of the amount of different water species as well as of self and cross H-bonding interactions. Construction and validation of suitable water sorption thermodynamic models against these experimental data supply an important tool for interpretation and quantification of the behaviour of a polymer matrix exposed to a humid environment.

In this chapter, the general issue of sorption thermodynamics of water in rubbery and glassy polymers is addressed, using a modelling approach which accounts for possible hydrogen bonding (HB) interactions and, in the case of glassy polymers, for the out-of-equilibrium state of the glassy system. It is illustrated how it is possible to investigate molecular interactions, evaluate the number of interacting species (penetrant–penetrant and polymer–polymer self interactions as well as

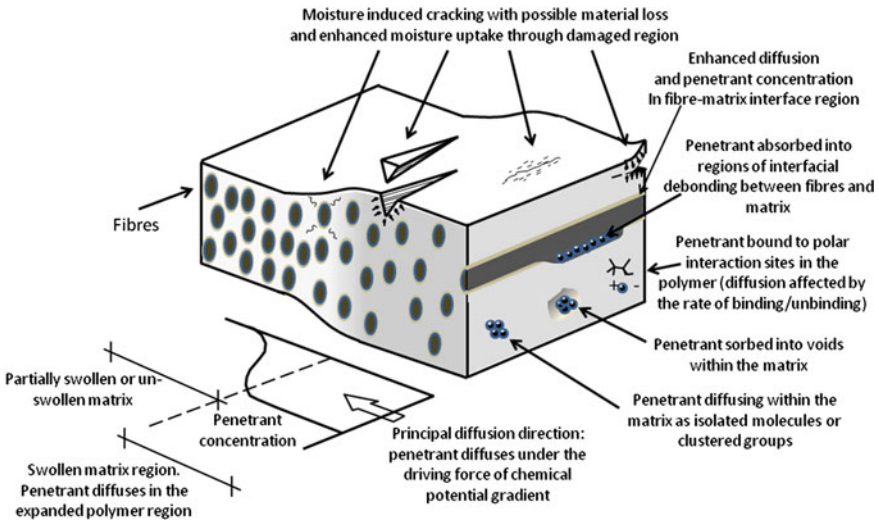

Fig. 1 Schematic illustration of possible moisture sorption locations and mechanisms (re-adapted from Ref. [2])

penetrant and polymer cross interactions) and quantify the relative amount of each interacting complex present at equilibrium state and during the transient sorption stage. Experimental and theoretical analyses are in fact combined to analyze sorption of water in rubbery (polycaprolactone, PCL) and glassy polymers (polyimides, with different degree of fluorination, epoxies and polyetheretherketone). In this manuscript, for the sake of brevity, attention is mainly focused upon thermodynamic aspects, without reporting the analysis of mass transport properties, which can also be performed using the same experimental tools.

2 Sorption Thermodynamics of Water in Polymer Matrices

2.1 Rubbery Polymers: The NRHB Model

Equation of state (EoS) approaches based on statistical thermodynamics provide a powerful framework to model thermodynamic properties and phase equilibria of mixtures of rubbery polymers and low molecular weight compounds (penetrants). A class of theoretical EoS models proposed is that grounded on compressible "mean field" lattice fluid theory (LF-EoS) [3–7]. However, these approaches are well suited only for systems where no specific interactions occur and, therefore, should not be used for polymer-water mixtures displaying Hydrogen Bondings (HB). To this aim, Panayiotou and Sanchez [8] have modified the original Sanchez-Lacombe LF-EoS theory [4–6] to account for the formation of possible self and cross HB in multicomponent systems. The mean field contribution adopted in their model (in the following PS model) is based on a simplified statistical framework, in which a random arrangement of r-mers and holes is assumed. Actually, in the case of non-athermal mean field contacts between different kind of r-mers and/or holes, such an assumption is likely to be incorrect. More recently, to overcome this intrinsic limitation of PS model, Panayiotou et al. developed the 'Non-Random lattice fluid Hydrogen Bonding' (NRHB) model [9–11] that is based on the factorization of the configurational partition function in two separate contributions: one related to mean field interactions and one accounting for the effects of specific HB interactions. The first contribution is constructed starting from the idea that the partition function related to mean field interactions can be further factorized into an ideal random contribution and a non-random contribution that is obtained treating each kind of contact as a reversible chemical reaction (i.e. the so-called *Quasichemical* approximation [12]). This latter contribution accounts for non-randomness of all the possible couple of contacts between mers of the components of the mixture as well as hole sites [13]. The second contribution, accounting for the effect of HB interactions, is formulated by using a combinatorial approach first proposed by Veytsman [14, 15], already adopted in the formulation of PS model.

We focus here on the phase equilibrium between a binary rubbery polymer-water mixture and pure water in a vapour phase, assuming that the polymer is not soluble within the gaseous phase. Therefore here we will consider only binary mixtures, with subscript '1' referring to water and subscript '2' referring to polymer. Establishment of this equilibrium implies the equality of the chemical potentials of water in the two coexisting phases. According to NRHB model, the general, non-equilibrium, expression of water chemical potential in the polymer-water mixture and in the pure water phase is expressed as sum of a LF and a HB contribution [10]:

$$\mu_1 = \mu_{1,LF} + \mu_{1,HB} \tag{1}$$

where

$$\begin{aligned}\frac{\mu_{1,LF}}{RT} = {} & \ln\frac{\phi_1}{\omega_1 r_1} - r_1\sum_{j=1}^{2}\frac{\phi_j l_j}{r_j} + \ln\tilde{\rho} + r_1(\tilde{v}-1)\ln(1-\tilde{\rho}) \\ & - \frac{z}{2}r_1\left[\tilde{v} - 1 + \frac{q_1}{r_1}\right]\ln\left[1 - \tilde{\rho} + \frac{q}{r}\tilde{\rho}\right] \\ & + \frac{zq_1}{2}\left[\ln\Gamma_{11} + \frac{r_1}{q_1}(\tilde{v}-1)\ln\Gamma_{00}\right] + r_1\frac{\tilde{P}\tilde{v}}{\tilde{T}} - \frac{q_1}{\tilde{T}_1} + \frac{\mu_{1,HB}}{RT}\end{aligned} \tag{2}$$

and

$$\frac{\mu_{1,HB}}{RT} = r_1 v_H - \sum_i^m d_i^1 \ln\left(\frac{v_d^i}{v_{i0}}\right) - \sum_j^n a_j^1 \ln\left(\frac{v_a^j}{v_{0j}}\right) \tag{3}$$

The reported expressions for LF and HB contributions to chemical potential are given in a general form which is valid for both pure penetrant in the gas phase and for penetrant in the binary polymer mixture. Refer to the fundamental literature on NRHB theory [9–11] for a detailed description of the relevant equations, of the parameters and of the variables, as well as of their corresponding symbols, which define the model as expressed by Eqs. 1–3.

In order to evaluate the equilibrium water chemical potential, the non equilibrium expressions (2) and (3) must be coupled with the proper expressions defining the equilibrium minimization conditions of Gibbs energy as a function of the internal state variables of the model [i.e. density, number of HB, number of site contacts; see points (b), (c) and (d) in the next paragraph], at fixed pressure, temperature and concentration.

In summary, the set of coupled non linear algebraic equations to be solved to determine the water solubility in a rubbery polymer according to the NRHB model is the following:

(a) equivalence of chemical potentials of water in the pure gas phase (μ_1^{GAS}) and in the polymer phase (μ_1^{POL}).

(b) Equations of State for the vapour and for the polymer mixture phases. The EoS in each phase formalizes the Gibbs energy minimization condition as a function of the internal state variable represented by the density. These equations solved simultaneously with the set of equations (a), (c) and (d) provide the density of the two phases at equilibrium.
(c) Equations formalizing the minimization condition of the Gibbs energy as a function of the set of internal state variable $\underline{N}_{ij}$ whose component *i*-*j* expresses the number of HB between proton donors of kind *i* and proton acceptors of kind *j* present in the phase investigated. These equations, solved simultaneously with the set of equations (a), (b) and (d) provide the number of the different kind of hydrogen bonds established in the two phases at equilibrium.
(d) Equations representing the Gibbs minimization condition as a function of the set of internal state variables $\underline{N}_{rs}^{NR}$ whose generic component *r*-*s* expresses the number of lattice contacts between mers of kind *r* and mers of kind *s* (including voids as tipology of mers). It is worth noting that the vector variable $\underline{N}_{rs}^{NR}$ contains only a subset of independent N_{rs}^{NR} as determined by the material balance equations (see Ref. [10]). In particular, the related internal state variables Γ_{00} and Γ_{11} appearing in the equations are, respectively, the non-random factors for the distribution of an empty site around another empty site and of molecular segments of penetrant around a molecular segment of the penetrant itself, in the two phases [10].

Relevant parameters of the model are:

1. k_{12}, (or, equivalently, $\psi_{12} = 1 - k_{12}$) that is the mean field lattice fluid interactional parameter which measures the departure of the mixing rule for the characteristic energies of the lattice fluid from the geometric mean:

$$\varepsilon_{12}^{*} = (1 - k_{12})\sqrt{\varepsilon_{11}^{*}\varepsilon_{22}^{*}} \tag{4}$$

2. E_{ij}^{0}, S_{ij}^{0} and V_{ij}^{0} representing, respectively, the molar internal energy of formation, the molar entropy of formation and the molar volume change upon formation of hydrogen bonding between the proton donor group of type *i* and the proton acceptor group of type *j* present in the system investigated.

It is important to note that the LF models, such as the NRHB theory, are in principle only suitable for totally amorphous rubbery polymer-penetrant mixtures and do not account for the presence of crystalline domains. For the sake of interpretation of experimental water sorption isotherms in semi-crystalline polymers whose amorphous phase is in a rubbery state—as is the case of water sorption in the semi-crystalline PCL in the present contribution—crystals can be modelled as being impervious to the penetrant and therefore the overall solubility is predicted by

rescaling the solubility of the pure amorphous phase to account for the presence of the crystalline fraction. The solubility in the amorphous phase is hence calculated using the approaches illustrated above, simply assuming that the presence of crystals does not alter the thermodynamic behaviour of the amorphous domains. Although this assumption could be considered questionable, it has been proven to be the most reliable choice as discussed in detail in the literature [16, 17].

In this contribution NRHB model has been adopted to investigate water sorption thermodynamics in semi-crystalline PCL.

2.2 Glassy Polymers: The NETGP-NRHB Model

Polymers in the glassy state display physical properties which significantly differ from those of the same polymer in the rubbery state. Consistently, also sorption thermodynamics differ substantially and modelling should properly account for non-equilibrium state. In particular, modelling thermodynamics of water sorption in glassy polymers displaying possible HB interactions is characterized by a twofold theoretical complexity: need to account for the out-of-equilibrium state of the glassy system and need to account for the occurrence of specific interactions.

A first successful and simple way to describe the sorption of penetrants within glassy polymers is represented by the so-called *Dual Sorption* model [18, 19]. Sorption of penetrants is assumed as being contributed by two 'populations': one is made of penetrant molecules molecularly dispersed in the bulk of polymer matrix, assumed to behave like an equilibrium rubbery system, and the other is made of penetrant molecules adsorbed onto the surfaces of the frozen micro-voids, which are intrinsically associated to the glassy state. Accordingly, the model is in the form of the sum of two contributions: the first is typically based on a mean field equilibrium approach, while the second one is in the form of a Langmuir-type adsorption contribution. In the case of interacting polymer-penetrant glassy systems (such as the case of water in hydrophilic polymers) the *Dual Sorption* model can be integrated with a second, additional, Langmuir's contribution accounting for the presence of specific adsorption sites where penetrant molecules establish interactions with chemical moieties present on polymer backbone.

Although rather successful in supplying a physically sound framework to interpret sorption in glassy polymers, *Dual Sorption* approach is suitable for correlation purposes but it is not predictive. Furthermore it does not account for the occurrence of possible penetrant clustering phenomena [20].

A more consistent approach is provided by a theoretical framework aimed at extending the equilibrium mixture theories suitable for rubbery polymers to the non-equilibrium glassy polymer-penetrant mixtures, by introducing internal state variables which act as *order parameters* quantifying the departure from the equilibrium conditions at fixed pressure and temperature. In this respect, Doghieri and Sarti [21, 22] have proposed the use, as *order parameter,* of the density of the polymer in the mixture and developed a procedure to extend equilibrium statistical

thermodynamics theories to non equilibrium glassy systems (the so-called NETGP model). Following this line of thought more recently Scherillo et al. have proposed [17, 23] the extension of NRHB theory to non equilibrium glassy systems to provide a suitable model for sorption of HB interacting penetrants in glassy polymers (the so-called NETGP-NRHB model). In the following we briefly report the development of NETGP-NRHB model referring to Ref. [17] for full details.

To extend to non-equilibrium the equilibrium statistical thermodynamics NRHB theory, it has been taken [21, 22] as non-equilibrium Gibbs energy the general expression derived for it from the developments of statistical thermodynamics, before the application of the minimization conditions that mark the equilibrium state. The constitutive class identifying the system, in the case of a spatially uniform phase, is considered to be the following set of variables: temperature (T), pressure (p), number of moles of penetrant (n_1), number of moles of polymer (n_2), density of the polymer in the mixture (ρ_2), set of number of HBs $\underline{N}_{ij}$ and set of effective number of nonrandom contacts $\underline{N}_{rs}^{NR}$. In such a case, the *internal state variables* to be selected for the description of the non-equilibrium state naturally emerge as the set of variables for which the minimization procedure is performed to obtain the equilibrium expression for G. In the case of NRHB model, ρ_2, $\underline{N}_{ij}$ and $\underline{N}_{rs}^{NR}$ can all be selected as *internal state variables* (see Ref. [17] for a more detailed discussion about the choice of possible *internal state variables* of the model). At equilibrium their value is only related to the equilibrium state variables through the minimization conditions for G mentioned in Sect. 2.1. Conversely, in non-equilibrium conditions, their values are dictated by the intrinsic evolution kinetics that, consistently with theory of *internal state variables*, must depend only on the actual state of the system.

Expressions for the evolution kinetics of the *internal state variables* hence need to be introduced. Regarding both the sets $\underline{N}_{ij}$ and $\underline{N}_{rs}^{NR}$ it is assumed, to simplify the matter, that an 'instantaneous' evolution kinetics holds for them. As a consequence, the HB contacts, $\underline{N}_{ij}$, and the non random contacts, $\underline{N}_{rs}^{NR}$, are the ones which the system would exhibit at equilibrium at the current values of pressure, temperature, number of moles of components and polymer density (this is referred as "instantaneous equilibrium" hypothesis, IE). In other words their values are obtained by using the minimization equations of points (c) and (d) of Sect. 2.1. With this assumption NETGP NRHB model formally displays the same constitutive class of the original NETGP theory of Doghieri et al. [21, 22] provided that the general non equilibrium expression of Gibbs energy is substituted by its IE form, i.e.:

$$\begin{aligned} G^{IE} &= g\left(T, p, n_1, n_2, \rho_2, \underline{N}_{rs}^{IE,NR}(T, p, n_1, n_2, \rho_2), \underline{N}_{ij}^{IE,HB}, (T, p, n_1, n_2, \rho_2)\right) \\ &= g^{IE}(T, p, n_1, n_2, \rho_2) \end{aligned} \tag{5}$$

Consistently, the rate of variation of ρ_2, which is a function of the state, becomes:

$$\begin{aligned}\frac{d\rho_2}{dt} &= f\left(T, p, \omega_1, \rho_2, \underline{N}_{rs}^{IE,NR}(T, p, \omega_1, \rho_2), \underline{N}_{ij}^{IE,HB}(T, p, \omega_1, \rho_2)\right) \\ &= f^{IE}(T, p, \omega_1, \rho_2)\end{aligned} \tag{6}$$

where ω_1 is the mass fraction of penetrant and the superscript IE in Eqs. (5) and (6) underlines that we are referring to the "instantaneous equilibrium" form for the dependence of $\underline{N}_{ij}$ and $\underline{N}_{rs}^{NR}$.

Although ρ_2 is, in the general formulation, a time dependent property characterized by a thermodynamically consistent kinetic expression [22], in the applications of the model to polymer systems well below glass transition temperature, it is frequently assumed that f takes a value close to zero due to the very slow relaxation kinetics of glassy polymers and ρ_2 is assumed to take a constant non-equilibrium value, referred to as $\rho_{2,\infty}$. This value has not to be confused with the equilibrium value, i.e. ρ_2^{EQ}, and it cannot be determined by using an equilibrium EoS. It is, hence, generally assumed that the polymer mixture is in a pseudo-equilibrium (PE) state for which:

$$\frac{d\rho_2}{dt} \cong 0 \tag{7}$$

$$\rho_2 = \rho_{2,\infty} \neq \rho_2^{EQ}(T, p, \omega_1) \tag{8}$$

For non-swelling penetrants $\rho_{2,\infty}$ can be simply considered as being equal to the value it takes for the pure polymer, ρ_2^0. Conversely, when penetrants induce a non negligible swelling, its value needs to be retrieved from dilation measurements on the mixture or, at low pressures, can be calculated using the simple expression [24]:

$$\rho_{2,\infty}(p) = \rho_2^0(1 - k_{sw}p) \tag{9}$$

where k_{sw} is the swelling coefficient, that can eventually be used as a fitting parameter for sorption isotherms. The kinetically hindered polymer-penetrant mixture, when in contact with an external phase of pure penetrant, reaches a phase pseudo-equilibrium (pseudo equilibrium attribute is used here since the mixture is itself in a pseudo-equilibrium glassy state). In the hypothesis that the polymer is insoluble in the external (*EXT*) penetrant phase, it can be demonstrated [22] that the thermodynamic condition for phase PE is still dictated by:

$$\mu_1^{POL}\left(T, p, \omega_1^{PE}, \rho_{2,\infty}\right) = \mu_1^{EXT}(T, p) \tag{10}$$

where the superscript PE has been used here to underline the fact that the value of the mass fraction of penetrant which satisfies the condition given by Eq. (10) is, actually, a PE value. The equilibrium penetrant potential in the pure external phase

μ_1^{EXT} is provided by the NRHB theory and, being an equilibrium value, it is only dependent upon T and p.

On the other hand, in view of the IE hypothesis it is possible to show (see Ref. [17] for details) that the expression for μ_1^{POL} is given by:

$$\begin{aligned}\frac{\mu_1^{POL}}{RT} &= \ln\frac{\phi_1}{\delta_1 r_1} - r_1\sum_{j=1}^{2}\frac{\phi_j l_j}{r_j} + \ln\tilde{\rho} + r_1(\tilde{v}-1)\ln(1-\tilde{\rho}) \\ &- \frac{z}{2}r_1\left[\tilde{v}-1+\frac{q_1}{r_1}\right]\ln\left[1-\tilde{\rho}+\frac{q}{r}\tilde{\rho}\right] \\ &+ \frac{zq_1}{2}\left[\ln\Gamma_{11}+\frac{r_1}{q_1}(\tilde{v}-1)\ln\Gamma_{00}\right] \\ &- \frac{q_1}{\tilde{T}_1} + \tilde{T}\left[\begin{array}{c}\ln(1-\tilde{\rho}) - \tilde{\rho}\left(\sum_i \phi_i\frac{l_i}{r_i}\right) \\ -\frac{z}{2}\ln\left(1-\tilde{\rho}+\frac{q}{r}\tilde{\rho}\right)+\frac{z}{2}\ln\Gamma_{00}\end{array}\right]\cdot\frac{rx_2\cdot\left.\frac{\partial\tilde{v}}{\partial x_1}\right|_{P,T,\rho_2,\underline{N}_{ij},\underline{N}_{rs}^{NR}}}{\tilde{T}} + \frac{\mu_{1,HB}^{POL,}}{RT}\end{aligned} \tag{11a}$$

where

$$\begin{aligned}\frac{\mu_{1,HB}^{POL}}{RT} &= r_1 v_H - \sum_i^m d_i^1\ln\left(\frac{v_d^i}{v_{i0}}\right) - \sum_j^n a_j^1\ln\left(\frac{v_a^j}{v_{0j}}\right) \\ &+ v_H\left.\frac{\partial\ln\tilde{v}}{\partial x_1}\right|_{P,T,\rho_2,\underline{N}_{ij},\underline{N}_{rs}^{NR}} x_2 r\end{aligned} \tag{11b}$$

It is worth noting that Eq. (11a) has to be calculated at $\rho_2 = \rho_{2,\infty}$.

In summary, the set of equations to be solved to predict, in PE conditions, sorption isotherms of a penetrant in a glassy polymer exhibiting HB interactions, is made of:

(a) equation expressing the equivalence of penetrant chemical potential in the gas phase (μ_1^{EXT}) and polymer phase (μ_1^{POL}).
(b) Minimization conditions for $\underline{N}_{ij}$ and $\underline{N}_{rs}^{NR}$ for the polymer phase and for the penetrant vapour phase.
(c) NRHB EoS for the vapour phase.

The model described in this section for the case of glassy polymers is suited only for amorphous polymers. As already discussed for the case of rubbery polymers, also in the case of semi-crystalline polymer-penetrant mixtures in which the amorphous phase is in a glassy state, it is assumed here that the overall PE solubility can be still predicted by simply rescaling the solubility of the pure amorphous phase to account for the presence of the crystalline fraction. It is hence hypothesized that only the crystalline and amorphous phases are present, neglecting the occurrence of

a third 'interphase'. In this respect it is worth noting that in the case of glassy systems the PE density $\rho_{2,\infty}$ to be used represents the one of the actual amorphous phase of the semi-crystalline polymer. As a first approximation, its value can be retrieved by information on the overall density of semi-crystalline polymer, once the degree of crystallinity and the density of the pure crystalline phase are available. An example of this procedure is illustrated in the section devoted to water sorption in semicrystalline PEEK.

In this contribution NETGP NRHB model has been adopted to investigate water sorption thermodynamics in amorphous glassy polyimides and in a semicrystalline PEEK. In the case of a glassy epoxy water sorption thermodynamics is only analysed experimentally in view of the unavailability of dilatometric data in the rubbery state, which are needed to determine the EoS parameters. This is due to chemical degradations occurring in these polymers at the high temperatures required to reach the equilibrium rubbery state.

2.3 Evaluation of Tg Depression

One of the most relevant physical effects of the presence of absorbed penetrants in glassy polymers is the decrease of T_g, a phenomenon that is known as *plasticization*. Although we will not discuss here any experimental data on T_g change promoted by water sorption, we think it is worth presenting theoretical developments on this issue related to the NRHB thermodynamic approach.

The first theories developed to predict the plasticization accounted only for the concentration of absorbed penetrant while more recent approaches, grounded on the EoS theories developed for the interpretation of sorption thermodynamics, account also for the effect of the mechanical action of pressure that, in some operative environments, can be quite high.

One of the first models for glass transition rooted on a thermodynamic framework is the theory of Gibbs and Di Marzio [25–27]. This LF theory assumes the occurrence of a true thermodynamic second order transition, for a fixed composition and pressure, at a temperature T_2 where the equilibrium configurational entropy of the system becomes equal to zero: at temperatures below or equal to T_2 the system is frozen in an out-of equilibrium state. The measurable T_g is higher than T_2: it is a kinetically affected, experimentally accessible, value for T_2 which represents the lower bound of the actually detectable T_g.

The criterion for the identification of the glass transition temperature for pure polymers and polymer-penetrant mixtures as the point at which the equilibrium configurational entropy becomes zero, can be extended to other thermodynamic models able to supply an expression for entropy. According to this line of thought the models of Chow [28], Gordon [29], and Ellis and Karasz [30–32] were developed. In a more recent series of papers [9, 33, 34] Panayiotou and co-workers used the NRHB lattice fluid model to calculate the entropy of pure amorphous polymers and of polymer-penetrant mixtures and, in turn, to evaluate T_g according

to the Gibbs–Di Marzio procedure. In order to perform the calculation of the T_g of the mixture, the flex energy of the pure polymer is needed. It can be typically calculated by equating the entropy of the pure polymer to zero at atmospheric pressure, if the T_g of the pure polymer is known. It is worth noting that the NRHB model accounts also for specific hydrogen bonding interactions and hence it has the distinctive feature of being able to supply an expression for T_g suited for systems displaying such specific interactions. This is a relevant result to the aim of assessing environmental resistance of composite matrices.

According to the NRHB model, the expression of the entropy of a polymer-penetrant mixtures can be expressed as the sum of three contributions:

$$S_{tot} = S_r + S_{nr} + S_{HB} \tag{12}$$

In the previous expression S_{tot} is the total configurational entropy of the system, S_r is a *randomicity* contribution, S_{nr} is a contribution related to *non-randomicity* of the site contacts in the lattice and S_{HB} is the hydrogen bonding contribution involved in the system. For a binary polymer-penetrant mixture, the NRHB non equilibrium expressions for these contributions are:

$$\begin{aligned} S_r/(RrN) = &\sum_{i=1}^{2}\left(\frac{\phi_i}{r_i}\right)\ln\delta_i + (1-\tilde{v})\ln(1-\tilde{\rho}) + (l+\ln(r\tilde{v}))/r \\ &- \sum_{i=1}^{2} x_i \ln x_i + (z/2)(\tilde{v}-1+q/r)(1-\tilde{\rho}+q/r) \end{aligned} \tag{13a}$$

$$\begin{aligned} S_{nr}/(RrN) = &(z/2)[-(\tilde{v}-1)\ln(\Gamma_{00}) - (q_1/r_1)\phi_1\ln(\Gamma_{11}) \\ &- (q_2/r_2)\phi_2\ln(\Gamma_{22}) + (\tilde{v}-1)(\Theta_1\Theta_r\ln(A_{01})\Gamma_{01} \\ &+ \Theta_2\Theta_r\ln(A_{02})\Gamma_{02}) + (q_1/r_1)\phi_1\Theta_2\Theta_r\ln(A_{12})\Gamma_{12}] \end{aligned} \tag{13b}$$

$$\begin{aligned} S_{HB}/(RrN) = &-\sum_{\alpha=1}^{m}\sum_{\beta=1}^{n}\upsilon_{\alpha\beta} - \sum_{\alpha=1}^{m}\upsilon_d^{\alpha}\ln\left(\frac{\upsilon_{\alpha o}}{\upsilon_d^{\alpha}}\right) \\ &- \sum_{\beta=1}^{m}\upsilon_a^{\beta}\ln\left(\frac{\upsilon_{0\beta}}{\upsilon_a^{\beta}}\right) + \left(\sum_{\alpha=1}^{m}\sum_{\beta=1}^{n}\upsilon_{\alpha\beta}H^0_{\alpha\beta}\right)/RT \end{aligned} \tag{13c}$$

In Eq. (13a)

$$\begin{aligned} \ln\delta_i = &\ln(Z) + f_i r_i \ln(Z-2) - f_i r_i \ln(f_i) \\ &- r_i(1-f_i)\ln(1-f_i) - f_i r_i u_i/(RT) \end{aligned} \tag{14a}$$

with

$$f_i = \frac{(Z-2)\exp(-u_i/(RT))}{(Z-2)\exp(-u_i/(RT)) + 1} \tag{14b}$$

where u_i represents the flex energy of bond i.

In order to obtain the expression for the equilibrium total configuration entropy the Eqs. (12–14b) must be coupled with the NRHB minimization equations reported in Sect. 2.1. For the complete description of the symbols in Eqs. (12–14b) the reader is referred to the relevant literature on NRHB [9–11]. Equation (13a) has been obtained by the authors of the present contribution in cooperation with prof. Tsivinzelis and it has been reported for first time in [35]. Note that Eq. (13c) is different from the corresponding expression erroneously reported, due to misprints, in the literature [35, 36].

In the case of crosslinked systems, a further term needs to be added to Eq. 13a–13c, i.e.:

$$S_{cross}/(RrN) = -\frac{3}{2}R\left(\frac{v_e}{M_2}\right)\phi_2\rho_2^*v^*\left(\alpha^2 + \frac{1}{\alpha^2} - 2 + \log\alpha\right) \tag{13d}$$

The theories illustrated so far are based on an equilibrium thermodynamics approach. Alternative models have been proposed rooted on molecular mobility arguments [37] based on the free volume theory originally developed by Turnbull and Cohen [38, 39].

A final point that is worth mentioning here concerns the effect of the presence of crystalline regions on the T_g of the amorphous phase. Actually, the crystalline regions place a constraint to the mobility of the amorphous phase and influence its conformational motions. As a consequence one cannot rule out the possibility that this constraint could affect the reliability the procedures illustrated above for the prediction of T_g change. This is a controversial point and it is expected that extension to semi-crystalline polymers of the models mentioned above is not a trivial task.

2.4 Combined Theoretical/Experimental Procedure

The theoretical approach illustrated in Sects. 2.1 and 2.2 has been used to analyze water sorption thermodynamics in several polymer systems in combination with experimental investigation based on vibrational spectroscopy and gravimetric measurements. A summary of the steps of the combined theoretical/experimental procedure is reported below:

1. The wealth of information available from FTIR in situ spectroscopy is used to identify proton donor and acceptor groups present on polymer backbone as well as the kinds of water species as distinguished by the number of hydrogen bonds they form in cross- and self-interactions.
2. Based on this information, model is tailored by specifying the number of possible types of HB interactions.
3. Once the model structure has been built up, gravimetric sorption isotherms data can be interpreted thus determining the mean field interaction parameter and the HB interaction parameters, by a fitting procedure.

4. At this stage the theoretical model is completely specified and can be used to provide a quantitative prediction of the amount of each type of HB interaction as a function of water vapour activity.
5. Self consistency of the thermodynamic theory can be hence assessed by comparing this prediction with results of the vibrational spectroscopy analysis. In fact, on the grounds of the results of 2D-COS as well as of quantitative elaboration of spectra based on determination of molar absorptivity of each water species derived from calibration against gravimetric data, an estimate of the amount of each type of HB interaction is provided.

Details of the experimental procedures are reported in the following sections.

2.4.1 In-Situ FTIR Time-Resolved Transmission Spectroscopy and 2D Correlation Spectroscopy

A custom built cell, operating at controlled relative humidity and temperature, was used to perform the time-resolved acquisition of FTIR spectra during the sorption experiments. The cell, positioned in the sample compartment of the spectrometer, was connected through service-lines, to a water reservoir, a turbo-molecular vacuum pump, and pressure transducers. Data collection on the polymer films exposed to water vapour at constant relative pressures (relative pressure, also referred to as relative humidity, is given by the ratio p/p_0, where p is the pressure of water vapour and p_0 is vapour pressure of water at the temperature of the test) was carried out in the transmission mode. A single data collection per spectrum was performed, which took 2.0 s to complete in the selected instrumental conditions. Full absorbance spectra (i.e. polymer plus absorbed water) were obtained using as background the cell without sample at the test conditions. The spectra representative of absorbed water were then obtained by using as background the single-beam spectrum of the cell containing the dry polymer film. This allows one to eliminate the interference of the polymer spectrum in the regions of interest. It is explicitly noted that this data processing approach is equivalent to the more general difference spectroscopy method provided that no changes in sample thickness take place during the measurement. Curve fitting analysis of difference spectra was performed by a Levenberg–Marquardt least-squares algorithm [40, 41]. The peak function used throughout was a mixed Gauss-Lorentz line shape.

2D-Correlation Spectroscopy (2D-COS) is a technique capable of improving the resolution by spreading the data over a second frequency axis. In particular, we have examined the asynchronous spectrum, that is characterized by the fact that a peak in this spectrum at $[\nu_1, \nu_2]$ corresponds to two IR signals changing at different rates. On the other hand, a zero intensity is obtained when two signals change at the same rate, thus providing the characteristic resolution enhancement and the specificity of the asynchronous pattern. Moreover, the sign of the asynchronous peaks supplies information about the sequence of changes of the two correlated IR

signals, according to the so-called Noda rules [42, 43]. In all the cases illustrated in this contribution, 2D-COS analysis was performed on an evenly spaced sequence of 20 spectra collected with a sampling interval of 12 s.

2.4.2 Gravimetric Analysis

Gravimetric water sorption isotherms were obtained using an electronic microbalance D200 from Cahn Instruments (Madison, WI) providing a sensitivity of 0.1 μg with an accuracy of ±0.2 μg. The weight gain of the sample exposed to a controlled humidity environment was determined as a function of time after each step increase of pressure of water vapour. Equilibrium sorption values were taken at each relative humidity as those attained by the sample after its weight remained constant for a time interval equal at least to twice the time needed to get to that value within ±0.4 μg.

3 Experimental and Theoretical Analysis of Different Systems

3.1 Glassy Polymers

3.1.1 Polyimide-Water System

Water sorption thermodynamics has been investigated in three glassy polyimides with an increasing amount of fluorine atoms in the polymer backbone, i.e. PMDA-ODA obtained by thermal imidization of its polyamic acid precursor, Pyre-ML RK692 from IST, Indian Orchard, MA (no F atoms, T_g = 383 °C). 6FDA-ODA (2 F atoms per repeating unit, T_g = 308 °C) and 6FDA-6FpDA (4 F atoms per repeating unit, T_g = 315 °C) obtained by thermal imidization of polyamic acid precursors which were synthesized from the respective dianhydride and diamine monomers [(hexahydrofluoroisopropylidene) diphthalic anhydride (6FDA), 4,4′-diaminodiphenyl ether (ODA), 4,4′-(hexafluoroisopropylidene) dianiline (6FpDA)], according to the procedures described in Ref. [44].

The suppression of the polymer matrix interference by use of difference spectroscopy, allows one to isolate the spectrum of absorbed water in the different environments. In the present context it is of particular interest the OH stretching region, ν_{OH}, of the spectrum of absorbed water (i.e. the 3,800 – 3,200 cm^{-1} region). The spectra reported in Fig. 2 evidence significant differences in terms of total absorbed water among the three investigated polyimides. As expected, the amount of absorbed water decreases considerably with increasing the fluorine content. The occurrence of distinct water species involved in H-bonding

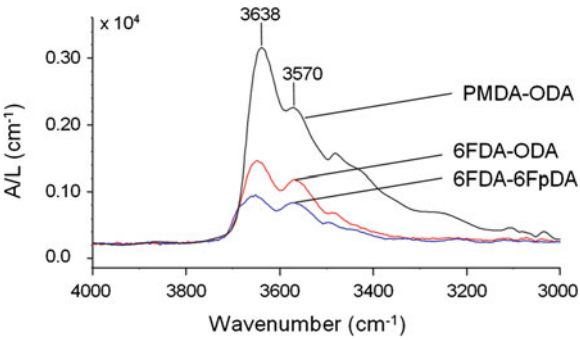

Fig. 2 Difference spectra (wet–dry) normalized for the sample thickness, representative of water absorbed in the three investigated polyimides. 4,000–3,000 cm^{-1} wavenumber range. Spectra denoted as wet were collected at equilibrium at $p/p_0 = 0.6$

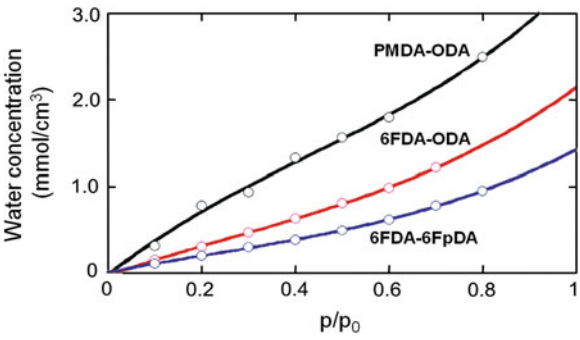

Fig. 3 Gravimetric water sorption isotherms for the three investigated polyimides. *Lines* represent only a guide for the eye

interactions is indicated by the fact that profiles display a complex, well-resolved band-shape.

Gravimetric sorption isotherms are reported in Fig. 3, confirming that the highest sorption capacity is shown by PMDA-ODA and the lowest by 6FDA-6FpDA. The upturn present in sorption isotherms at high relative pressure is likely due to the gradual onset of penetrant clustering or self-association, as will be confirmed by the analysis of spectroscopic data.

The correlations between the absorbance area of the ν(OH) band and the water concentration evaluated gravimetrically show that the three data sets can be accommodated on a single master curve, after absorbance normalization for sample thickness [45]. A significant departure from linearity (presence of an upturn) in this correlation is observed for concentration values exceeding 0.75 mmol/cm^3. The very high correlation degree between the spectroscopic and gravimetric data relative to the three polyimides for the stretching frequency range, points to the conclusion that for this vibrational mode the absorptivity values of the different water species are independent of the particular polyimide system. The mentioned upturn at higher values of water concentration qualitatively indicates an increase in the relative concentration of water species characterized by higher absorptivity values.

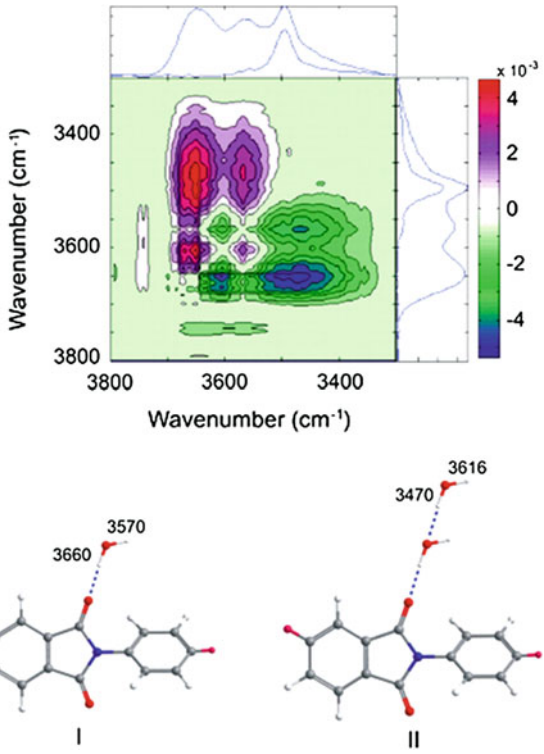

Fig. 4 *Top* 2D-FTIR correlation spectra (asynchronous) obtained from the time-resolved spectra collected during water sorption in 6FDA-ODA polyimide at a relative pressure = 0.6. *Bottom* Schematic representation of the H-bonding interactions in the investigated water/6FDA-ODA system (schemes I and II)

To elucidate the number and types of absorbed water species, 2D-COS has been performed on the three sets of data [45]. An example of correlation spectra as calculated for the case of 6FDA-ODA, is reported in Fig. 4. From the 2D results obtained from the elaboration of the spectra collected for the three investigated polyimides, it is found the presence of two couples of signals: one at 3,660 – 3,570 cm^{-1} and one at 3,616 – 3,456 cm^{-1}. The two components of each couple change at the same rate, but the two couples exhibit a different dynamics. These results can be interpreted by assuming that two different water species occur. While this pattern is common to both PMDA-ODA and 6FDA.ODA, in the case of 6FDA-6FpDA two additional correlation peaks are found indicating the presence of a further component at 3,700 cm^{-1}. The vibrational assignment of the identified signals can be performed only after the identification of interaction sites active on the macromolecule. A detailed analysis [45] of vibrational spectroscopy results indicated that the imide carbonyls are involved in HB interactions as proton acceptor groups, while the involvement of ether group (in the case of PMDA-ODA and 6FDA-ODA) as proton acceptor in H-bonding can be safely neglected.

On the basis of these findings, one can propose likely structures for the H-bonding aggregates that are formed in the investigated systems. In fact, the couple of water signals at 3,660 – 3,570 cm^{-1}, identified in all the three polyimides, can be

associated, respectively, to the out-of-phase and in-phase stretching modes of water molecules bound to imide carbonyls via a H-bonding interaction (see structure I in Fig. 4). The two peaks, present in all the three polyimides at 3,616 and 3,470 cm^{-1}, can be associated to self-associated water in the prevalent form of dimers (see structure II in Fig. 4). Concerning the signal identified only for 6FDA-6FpDA no definitive assignment can be provided. A detailed discussion on this point is available in [45].

With the aim of quantifying the concentration of the different water species, attention has been focused on ν_{OH} range. In particular two analytical peaks characteristic of the species to be quantified, i.e., at around 3,568 cm^{-1} for the monomer and at 3,495 cm^{-1} for the dimer, have been chosen.

The total integrated absorbance, A_{TOT}, in the ν_{OH} range can be expressed as:

$$\frac{A_{TOT}}{L} = \sum_{i=1}^{N} \varepsilon_i C_i \tag{14}$$

where C_i is the molar concentration of the i-th component, ε_i is the associated molar absorptivity, L is the sample thickness, and N represents the number (two, in the case at hand) of individual components in which the experimental profile has been decomposed. By interpreting the experimental data for $\frac{A_{TOT}}{L} = \frac{A_{3,568}+A_{3,495}}{L}$ as a function of total water concentration, an estimate of the values of molar absorptivities can be obtained, thus allowing the evaluation of the concentration of each species.

With the aim of comparing these results with the predictions of the NETGP–NRHB model, these data have been re-elaborated to convert the concentration of the different water species into the outcome of the model, that is the number of self- and cross-HB established within the polymer–water mixture. In particular, we have calculated the number of moles of self-HB of water normalized per mass of polymer (n_{11}^{wp}/m_2, where m_2 represents the mass of polymer) and the number of moles of cross HB occurring between the proton donor groups of water molecules and the proton acceptor groups present on the polymer backbone, normalized per mass of polymer (n_{12}^{wp}/m_2). The calculation is rather straightforward in the case of dimeric water: in fact a 1:1 ratio can be safely assumed between the number of water molecules forming the "second shell" and the number of self-HB that they establish with water molecules interacting with carbonyls. In the case of water molecules bound to carbonyls, it has been assumed a single water molecule to form two H-bonding interactions with two distinct carbonyls (i.e., a 1:2 stoichiometry), thus "bridging" two functional groups. This bridging is statistically favoured as compared to the 1:1 stoichiometry due to the large excess of carbonyl groups with respect to absorbed water. This picture is supported by a spectroscopic investigation performed by Iwamoto and Masuda [46] proving that in polymers characterized by a dense distribution of carbonyl groups, like poly vinyl acetate (PVAc) and poly methyl methacrylate (PMMA), dissolved water is generally

hydrogen bonded through each OH to two C=O. Data re-elaborated in the form of normalized amount of cross- and self-HB are reported in Fig. 5.

Gravimetric sorption isotherms have been then interpreted with NETGP-NRHB model. To this aim, scaling parameters of NRHB equation of state for pure polymers (i.e. ε_h^*, ε_s^* and $v_{sp,0}^*$) have been first determined by fitting experimental PVT data at high pressures (up to 2,000 atm) in the rubbery state (see [17]). This analysis was possible only in the case of 6FDA-ODA and 6FDA-6FpDA (results reported in Table 1) since in the case of PMDA-ODA degradation occurs in the proximity of its glass transition temperature, thus making it impossible to perform PVT characterization in the rubbery state. As a consequence, the comparison between NETGP-NRHB model and spectroscopic data(see Fig. 5) was limited to the case of fluorinated polyimides. For the case of water, the three LF scaling parameters and the two hydrogen bonding parameters have been taken from literature [47] and are reported in Table 1 as well.

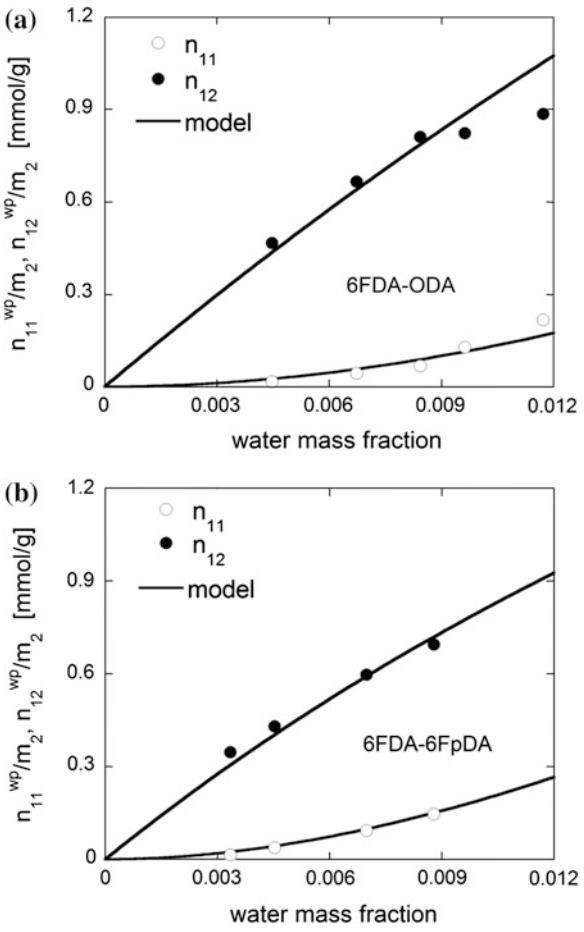

Fig. 5 Comparison of predictions of NETGP–NRHB model with experimental results for (*top*) 6FDA-ODA and (*bottom*) 6FDA-6FpDA

Table 1 NRHB parameters for pure polymides and pure water

Component	ε_s^* (J/mol)	ε_h^* (J/mol K)	$v_{sp,0}^*$ (cm^3/g)	E_{11}^{0w} (J/mol)	S_{11}^{0w} (J/mol K)	V_{11}^{0w} (cm^3/mol)	S
6FDA-ODA	5,988.5	4.3186	0.5736			–	0.7802[b]
6FDA-6FpDA	5,471.1	3.8652	0.5174			–	0.7757[b]
Water[a]	5,336.5	−6.506	0.9703	−16,100	−14.7	0	0.8610

[a] From Ref. [47]

[b] Calculated using group contribution calculation scheme UNIFAC (see Ref. [48, 49])

In the implementation of NETGP–NRHB model, in view of the small amount of absorbed water, the swelling coefficient, k_{sw}, has been taken equal to zero. Furthermore, following the assumptions made by Tsivintzelis et al. [47] $V_{11}^{0,wp}$ and $V_{12}^{0,wp}$ have been both taken as being equal to zero. Only two fitting parameters are then needed to model water sorption isotherms, i.e. the mean-field polyimide/water interaction parameter, $\psi_{12} = 1 - k_{12}$, and the molar Helmholtz energy of formation of polymer/water HB interaction, $A_{12}^{0,wp}$. In fact, since sorption data were taken only at one temperature (30 °C), it is not possible to separate the contributions of molar internal energy of formation of cross-HB interaction from the entropic one. Both these parameters are lumped in $A_{12}^{0,wp}$.

It is explicitly noted that, based on the spectroscopic findings, four proton acceptor groups (i.e., carbonyl groups) per repeating unit have been assumed to be present on the polymer backbone while two equivalent proton donor groups and two equivalent proton acceptor groups to be present on each molecule of water [10]. The NETGP–NRHB model supplies a good fitting capability of water sorption isotherms in both 6FDA-ODA and 6FDA-6FpDA. In Fig. 6 is reported

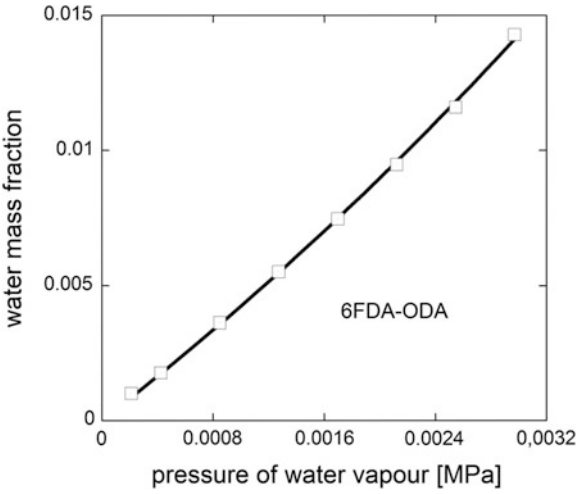

Fig. 6 Fitting of experimental water sorption isotherms for 6FDA–ODA. Continuous line represents fitting curve provided by NETGP–NRHB model

Table 2 NETGP-NRHB parameters for polyimide-water mixtures as obtained from data fitting of experimental sorption isotherms

System	ψ_{12}	A_{12}^{0wp} (J/mol)
6FDA-ODA/water	0.787	−12,400
6FDA-6FpDA/water	0.869	−12,100

the case of water sorption isotherm in 6FDA-ODA. The calculated values for best fitting parameters are reported in Table 2.

3.1.2 PEEK-Water System

Nominally amorphous PEEK films (Goodfellow Co., PA, USA) with a thickness of 12.5 μm were used in this investigation. A crystalline degree, χ_c, equal to 0.057 has been actually estimated on the basis of differential scanning calorimetry using information on enthalpy of melting available in [50]. This value has been used to scale the overall water solubility evaluated gravimetrically at different temperatures and relative humidity values, in order to obtain water solubility value referred to the sole amorphous phase. Also in this case, the NETGP-NRHB model has been used to interpret sorption thermodynamics of water in amorphous PEEK. To this aim, the "frozen" polymer density of the glassy amorphous phase of the polymer in the mixture was taken equal to that of the amorphous phase of pure polymer, $\rho_{2\,am}^0$, since no significant swelling is induced by water in view of the low concentration.

The density of the amorphous phase, ρ_{2am}^0, at 27.2 °C has been estimated to be 1.2695, using Eq. (15) that has been derived on the basis of the assumption that the volume of the semi-crystalline PEEK is the sum of those of the amorphous and crystalline phases i.e.:

$$\frac{1}{\rho_{2am}^0} = \frac{1}{(1-\chi_c)}\left(\frac{1}{\rho_2^0} - \chi_c \frac{1}{\rho_{2cr}^0}\right) \tag{15}$$

The theoretical value of density of pure crystalline phase ρ_{2cr}^0, has been taken equal to 1.400 (g/cm^3) from Ref. [51], while the overall density of the semicrystalline sample, ρ_2^0, has been evaluated to be 1.2763 g/cm^3 by Helium picnometry performed at 27.2 °C.

The values of ρ_{2am}^0 at the four temperatures at which the water sorption thermodynamics has been investigated (30, 45, 60 and 70 °C), have been then calculated, starting from its value at 27.2 °C, on the basis of the thermal expansion coefficient of the amorphous PEEK taken from Ref. [52] and are reported in Table 3.

In defining the relevant HB interactions occurring in the system to be used in the NETGP-NRHB approach, it has been assumed that self HB interaction take place only between water molecules involving the two proton donor groups and

Table 3 Densities (g/cm^3) of the amorphous phase of the investigated PEEK at the four temperatures of interest

T = 30 °C	T = 45 °C	T = 60 °C	T = 70 °C
1.2688 ± 0.001	1.2652 ± 0.001	1.2617 ± 0.001	1.2593 ± 0.001

Table 4 NRHB parameters for PEEK

Component	ε_s^* (J/mol)	ε_h^* (J/mol K)	$v_{sp,0}^*$ (cm^3/g)	s
PEEK	6,401	4.003	0.7351	0.7151[a]

[a] Calculated using group contribution calculation scheme UNIFAC (see Ref. [48, 49])

the two proton acceptor groups, present on each water molecule. Conversely, cross HB interactions are assumed to take place only between water proton donor groups and the carbonyl group located on the PEEK backbone (one for each repeating unit), even though water interaction with the ether oxygen on the polymer repeating unit cannot be presently ruled out. The LF and the self HB parameters associated to the pure components are reported in Table 4. In particular the values of ε_s^*, ε_h^* and $v_{sp,0}^*$ for PEEK have been obtained by best fitting high pressure dilatometric data (PVT data) of PEEK in the equilibrium molten state at different temperatures and pressures available in the literature [53].

Simultaneous data fitting of the four experimental sorption isotherms investigated has been performed (see Fig. 7) and the three corresponding best fitting parameters obtained are reported in Table 5. As it is evident from Fig. 7, the NETGP-NRHB model provides a good quality of fitting of equilibrium sorption isotherms of water in PEEK. In particular the self HB contribution term allows to correctly describe the upward concavity exhibited by the curves, particularly at high vapour water activity.

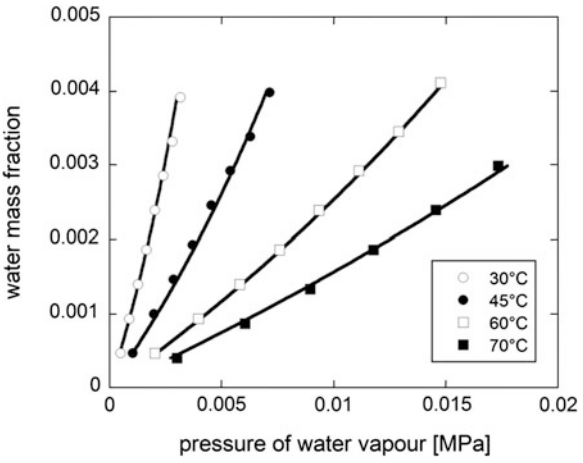

Fig. 7 Fitting of experimental water sorption isotherms for PEEK expressed as water mass fraction in the amorphous phase as a function pressure of vapour water. *Continuous lines* represent fitting curves provided by NETGP-NRHB model

Table 5 PEEK-water mixture NETGP-NRHB parameters as obtained from data fitting of experimental sorption isotherms. V_{12}^{0wp} has been assumed as being equal to 0 and does not result from fitting

ψ_{12}	E_{12}^{0wp} (J/mol)	S_{12}^{0wp} (J/mol K)	V_{12}^{0wp} (cm^3/mol)
1.023	−14,376	−13.14	0

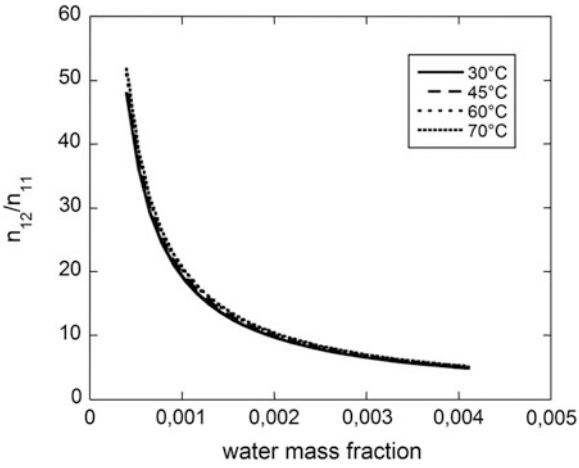

Fig. 8 Predicted values of the ratio of water self-HB and water-PEEK cross-HB, all reported as a function of water mass fraction in the PEEK amorphous phase, at 30, 45, 60 and 70 °C

As for the case of polyimides, once the optimized parameters have been determined by the fitting procedure, NETGP-NRHB model can be used to predict the amounts of self (i.e.1–1) and cross (i.e. 1–2) HB interactions occurring in the PEEK-water mixtures at the four temperatures investigated. In Fig. 8 is reported, in particular, the predicted values for the ratio n_{11}^{wp}/n_{12}^{wp} as a function of water mass fraction in the amorphous phase of PEEK. As for the case of polyimides-water systems illustrated before, at low water concentration cross-HB interactions prevail while the water self-HB interactions increase their relative importance as total water concentration increases. Vibrational spectroscopy analysis is in progress in order to provide a quantitative experimental estimate of the amount of each kind of HB interactions to be compared with model predictions.

3.1.3 Epoxy-Water System

The analysis of sorption thermodynamics of water has been performed also for epoxy resins. We present here the case of tetraglycidyl 4,4′-diaminodiphenyl methane–4,4′-diaminodiphenylsulfone (TGDDM-DDS) resin that was actually the first polymer-water system investigated by our group exploiting the wealth of information available from in situ vibrational spectroscopy. Water sorption

thermodynamics have been interpreted in the light of self- and cross-HB. The experimental results reported here are obtained at 24 °C.

Due to the higher complexity of chemical structure of this system as compared to PIs and PEEK, the theoretical interpretation of sorption thermodynamics has been based on a phenomenological model [54]. The procedures adopted for the experimental spectroscopic and gravimetric investigation and of consequent data elaboration and analysis are identical to those adopted in the case of PIs. However, 2D-COS analysis was not performed since it was not yet fully developed as a data elaboration tool at the time of the investigation.

Making use of difference spectroscopy, the spectrum of absorbed water in the ν_{OH} region has been isolated by eliminating the interference of the hydroxyl groups of the epoxy resin. The analysis has been performed during sorption of water and at sorption equilibrium at several values of relative pressure of water vapour. The collected difference spectra convey important information not only on the state of water molecules but also on the perturbation of the vibrational modes of the epoxy network. In fact peak shifts and/or intensity changes occur as a consequence of the interactions with water, thus allowing the identification of the interacting groups of the network.

An example of a sequence of subtraction spectra collected water in the ν_{OH} region during a sorption test relative to different sorption times, and hence, to different concentrations of water in the sample, is reported in Fig. 9 for the sorption test performed at $p/p_0 = 0.4$. A complex band due to the ν_{OH} modes of absorbed water is observed. In particular, a high frequency peak is identified at 3,610 cm^{-1}, partly superimposed on a much broader absorption located around 3,370 cm^{-1}. We anticipate that the 3,610 cm^{-1} component is due to non-interacting water molecules, while the 3,370 cm^{-1} band arises from H-bonded water species.

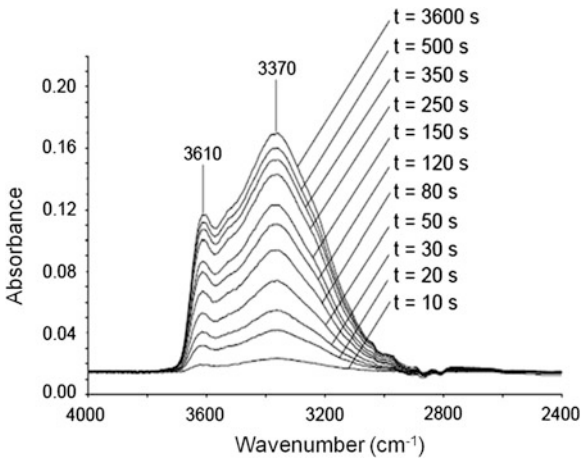

Fig. 9 Subtraction FTIR spectra collected for the system water/TGDDM-DDs at different sorption times at $p/p_0 = 0.4$. Frequency range 4,000–2,300 cm^{-1}

Concerning peaks associated to the epoxy network, we notice the displacement towards lower frequencies, upon water sorption, of the peaks located at 1,720 and 1,670 cm^{-1} in the spectrum of the dry resin. These peaks are associated to carbonyl groups (aldehydes and/or ketones at 1,720 cm^{-1} and amide groups at 1,670 cm^{-1}). This effect indicates the involvement of these carbonyls as proton acceptors in H-bonding interaction with water. However, owing to the reduced concentration of the above groups, this kind of interaction is likely to represent a relatively minor fraction of bonded species Another shift occurring upon sorption is that of the peak centred at 1,594 cm^{-1} in the dry resin. This displacement is likely to be related to the involvement of residual secondary amine groups in molecular interactions with water. The observation that the shift occurs towards lower wavenumbers is suggestive of the fact that, in this specific interactional configuration, the nitrogen is involved as a proton acceptor. Finally, displacements upon sorption are also observed for the peaks at 1,290 and 1,145 cm^{-1}, which originate from the out-of-phase and in-phase stretching modes of the sulphone groups. The downward shift of both peaks upon water absorption definitively confirms the involvement of these groups as proton acceptors in H-bonding interactions with the penetrant.

A more detailed analysis of the ν_{OH} region (4,000–2,600 cm^{-1}) by applying a least squares curve-fitting algorithm, allows to resolve the complex spectral profiles of Fig. 9 in their component peaks. This provides additional information about the different water species and their relative populations. The results of such an analysis in the 4,000–2,600 cm^{-1} range evidence the presence of four peaks. The assignments of these peaks are discussed in [54, 55]. In particular, the high frequency peak at 3,623 cm^{-1} is related to the asymmetric O–H stretching vibration (ν_{as}) of unassociated water (i.e. water which does not establish any H-bond, S_0), while the component at 3,555 cm^{-1} can be related to singly H-bonded molecules (S_1). Moreover, the two components at 3,414 and 3,272 cm^{-1} (respectively S'_2 and S''_2) arise from the S_2 species interacting with the sulphone and the amino-alcohol groups. In view of the stronger H-bonding capability of the amino-alcohol group with respect to the sulphone, the 3,272 cm^{-1} peak is assigned to the complexes (a) and (b) and the 3,414 cm^{-1} peak to the structure represented in by complex (c) in Scheme 1.

Based on $\Delta\nu$–$\Delta\varepsilon$ correlation and on the results of investigation by NIR analysis an estimation of the absolute values of absorptivity for the different water species present in the system id possible [54]. In fact, a fully spectroscopic estimate of the total concentration of absorbed water and of the concentration of each species can be obtained. In Fig. 10 are reported the concentrations of each water species as a function of total water concentration in TGDDM-DDS as determined at sorption equilibrium for several values of p/p_0 (i.e. 0.08, 0.2, 0.4 and 0.6). The linear dependence evident in all cases, implies the invariance of the molar fraction of each species with concentration, which points to a linear equilibrium between them. Furthermore, it is found that, at any concentration of absorbed water the prevailing species is S_2, which accounts for 53 % of the total.

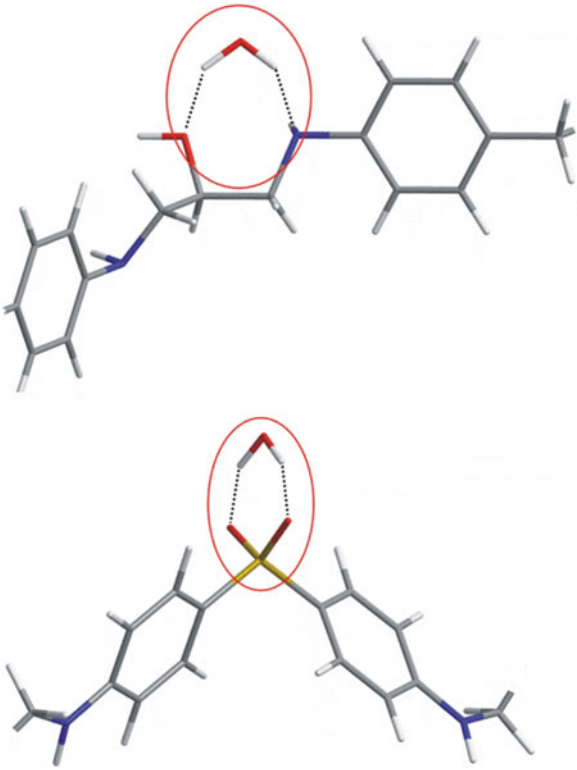

Scheme 1 Interactional complexes identified for double H-bonded water molecules (S_2 species) for the TGDDM-DDS/water system

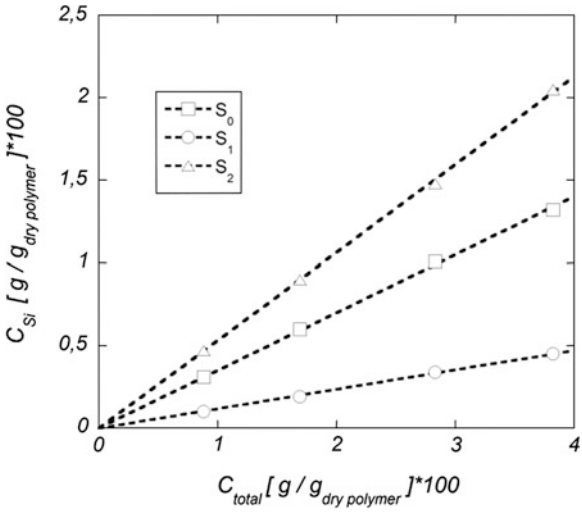

Fig. 10 Concentration of S_0, S_1, and S_2 water species reported as a function of total water concentration at sorption equilibrium n

As already pointed out, in the case of the TGDDM-DDS system no comparison was performed of the results of vibrational spectroscopy analysis with theoretical lattice fluid thermodynamic models, in view of unavailability of EoS parameters for the epoxy resin.

3.2 Rubbery Polymers

3.2.1 PCL-Water System

Experimental analysis of water sorption, by conducting gravimetric and vibrational spectroscopy experiments, has been performed also on thermoplastic polymers. In particular, we report here some recent results [23] for the system polycaprolactone-water. The results of combined gravimetric and vibrational spectroscopy analyses are compared with predictions of equilibrium NRHB model in terms of amount of water sorbed and number of self- and cross-HB. For the PCL/water system the results of 2D correlation spectroscopy are reported in Fig. 11 along with a schematic representation of self- and cross-HB interactions. In fact, only two species of water molecules have been detected: (a) water molecules HB-bonded to carbonyl groups of the polymer by cross-interactions (ether oxygen has been proven [23] not to be involved in any significant interaction with water); (b) water molecules HB-bonded by self-interaction to water molecules bonded to carbonyls.

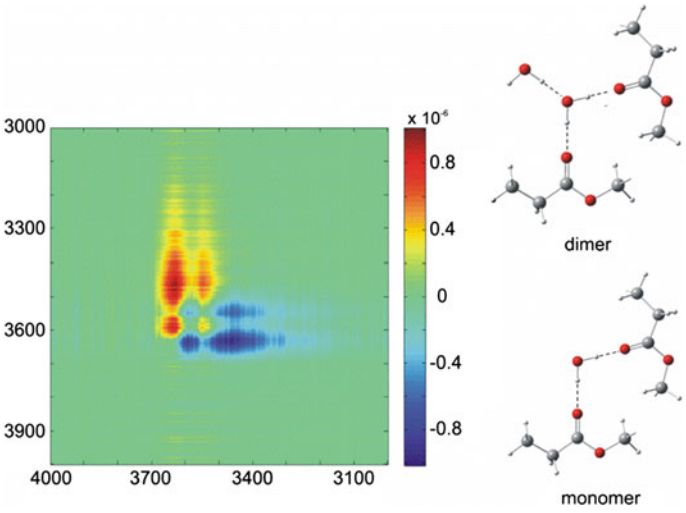

Fig. 11 *Left* 2D-FTIR correlation spectra (asynchronous) obtained from the time-resolved spectra collected during water sorption in PCL at relative pressure = 0.4. *Right* Schematic representation of the HB interactions

Adopting procedures similar to those used for polyimides, a quantitative assessment of the concentration of each water species and, in turn, of each type of HB-bond established (i.e. self- and cross-HB) has been obtained from spectroscopic data. It is worth mentioning that, in evaluating the amount of each HB interaction from each type of water species, it has been assumed, as already illustrated for the case of polyimides and based on similar arguments, that each water molecule interacting with polymer backbone actually establishes a bond with two carbonyls, thus 'brindging' two different polymer segments. Experimental gravimetric sorption isotherms at three temperatures are reported in Fig. 12. Experimental data have been normalized to the amorphous fraction of PCL, hence water mass fraction is referred to the mass of amorphous PCL. These data have been successfully interpreted using NRHB lattice theory (see continuous lines in the same figure). In Table 6 are reported the NRHB-EoS parameters, as determined from PVT measurements [23] for pure PCL. In Table 7 are reported the NRHB mean-field interaction parameter and cross-HB parameters for the PCL-water system obtained from data fitting of experimental sorption isotherms.

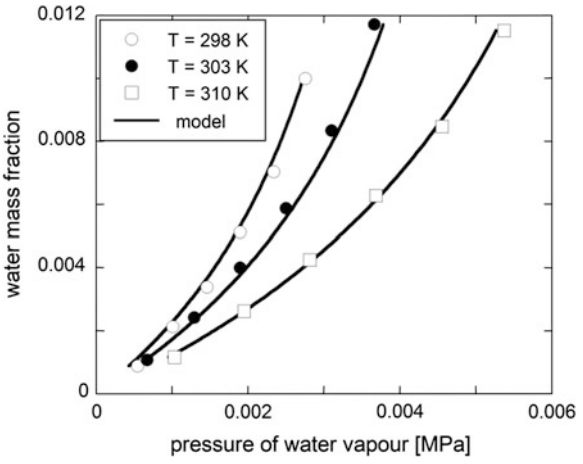

Fig. 12 Fitting of experimental water sorption isotherms for PCL expressed as water mass fraction in the amorphous phase as a function pressure of water vapour. *Continuous lines* represent fitting curves provided by NRHB model

Table 6 NRHB parameters for PCL

Component	ε_s^* (J/mol)	ε_h^* (J/mol K)	$v_{sp,0}^*$ (cm^3/g)
PCL	5876 ± 50	3.824 ± 0.01	0.8873 ± 0.005

Table 7 PCL-water mixture NRHB parameters as obtained from data fitting of experimental sorption isotherms. V_{12}^{0wp} has been assumed as being equal to 0 and does not result from fitting

ψ_{12}	E_{12}^{0wp} (J/mol)	S_{12}^{0wp} (J/mol K)	V_{12}^{0wp} (cm^3/mol)
1.115 ± 0.001	−11,130 ± 200	−6.13 ± 0.01	0

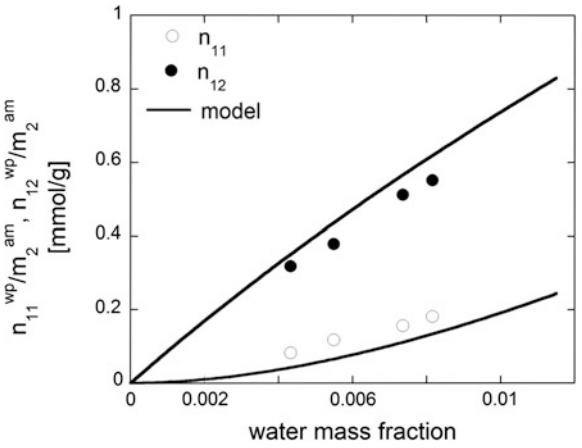

Fig. 13 Comparison of predictions of NRHB model (*continuous lines*) with experimental results for PCL-water system. Moles of water self-HB and moles of HB between absorbed water molecules and proton acceptor groups on the polymer backbone in the polymer/water mixture are per gram of dry amorphous PCL-Water mass fraction is referred to amorphous PCL

The NRHB model has been then used to predict the amount of cross- and self-HB established in the PCL-water system. As can be deduced from Fig. 13, NRHB model provides a good quantitative estimate for the number of self- and cross-HB.

4 Conclusions

Thermodynamic models for polymer-water mixtures based on non random lattice fluid EoS theories accounting for HB interactions has been proven to provide a consistent framework for the interpretation of water sorption in interacting rubbery and glassy polymers.

In fact, prediction of NRHB and of NETGP-NRHB models, respectively in the case of interacting rubbery and glassy polymers, compare well with the results of combined vibrational spectroscopy and gravimetric experimental analyses. In particular, a quantitative agreement between model predictions and experimental data has been obtained for the amount of self- and cross-HB established in poyimides and in PCL.

This approach paves the way to the interpretation of other important aspects associated with ingress of water in polymer matrices, including plasticization phenomena. In fact, an advantage of using an approach based on EoS theories for the description of sorption thermodynamics, is the availability of expressions for Gibbs energy and entropy of the polymer/water mixture that enables the easy implementation of the calculation of water effects on T_g of the system following approaches based on entropic arguments.

On the experimental side, we underline the wealth of information available on several kinds of polymer-water systems by performing on-line in situ FTIR spectroscopy coupled with analysis of 2D correlation spectra. This approach has proven to be a valuable tool to gather important information on (1) the type of

molecular interactions; (2) the interaction site(s) on the polymer backbone (3) the nature and the number of the penetrant species and, above all, (4) a method to quantitatively estimate the population of the different species present in the system.

References

1. Mensitieri G, Iannone M (2998) Modelling accelerated ageing in polymer composites. In: Martin R (ed) Ageing of composites. 1st edn. Woodhead Publishing Ltd, Cambridge (England), CRC Press, Boca Raton FL
2. Bond DA, Smith PA (2006) Modeling the transport of low-molecular-weight penetrants within polymer matrix composites. Appl Mech Rev 59:249–268
3. Flory PJ, Orwell A, Vrij RA (1964) Statistical thermodynamics of chain molecule liquids. J Am Chem Soc 86:3507–3514
4. Sanchez IC, Lacombe RH (1976) An elementary molecular theory of classical fluids. Pure fluids. J Phys Chem 80:2352–2362
5. Sanchez IC, Lacombe RH (1976) Statistical thermodynamics of fluid mixtures. J Phys Chem 80:2568–2580
6. Sanchez IC, Lacombe RH (1978) Statistical thermodynamics of polymer solution. Macromolecules 11:1145–1156
7. Simha R, Somcynsky T (1969) On the statistical thermodynamics of spherical and chain molecule fluids. Macromolecules 2:342–350
8. Panayiotou C, Sanchez IC (1991) Hydrogen bonding in fluids: an equation-of-state approach. J Phys Chem 95:10090–10097
9. Panayiotou C, Pantoula M, Stefanis E, Tsivintzelis I, Economou IG (2004) Nonrandom hydrogen-bonding model of fluids and their mixtures. 1. Pure fluids. Ind Eng Chem Res 43:6592–6606
10. Panayiotou C, Tsivintzelis I, Economou IG (2007) Nonrandom hydrogen-bonding model of fluids and their mixtures. 2. Multicomponent mixtures. Ind Eng Chem Res 46:2628–2636
11. Panayiotou CG (2009) Hydrogen bonding and nonrandomness in solution thermodynamics. In: Birdi KS (ed) Handbook of surface and colloid chemistry, 3rd edn. CRC Press, Taylor and Francis group, New York
12. Prausnitz JM, Lichrenthaler RN, Gomes de Azevedo E (1998) Molecular thermodynamics of fluid-phase equilibria, 3rd edn. Prentice Hall PTR, New Jersey
13. Taimoori M, Panayiotou C (2001) The non-random distribution of free volume in fluids: non-polar systems. Fluid Phase Equilib 192:155–169
14. Veytsman BA (1990) Are lattice models valid for fluids with hydrogen bonds? J Phys Chem 94:8499–8500
15. Veytsman BA (1998) Equation of state for hydrogen-bonded systems. J Phys Chem B 102:7515–7517
16. Bonavoglia B, Storti G, Morbidelli M (2006) Modeling of the sorption and swelling behavior of semicrystalline polymers in supercritical CO_2. Ind Eng Chem Res 45:1183–1200
17. Scherillo G, Sanguigno L, Galizia M, Lavorgna M, Musto P, Mensitieri G (2012) Non-equilibrium compressible lattice theories accounting for hydrogen bonding interactions: modelling water sorption thermodynamics in fluorinated polyimides. Fluid Phase Equilib 334:166–188
18. Barrer RM, Barrie JA, Slater J (1958) Sorption and diffusion in ethyl cellulose. Part III. Comparison between ethyl cellulose and rubber. J Polym Sci 27:177–197
19. Michaels AS, Vieth WR, Barrie JA (1963) Solution of gases in polyethylene terephthalate. J Appl Phys 34:1–12

20. Mensitieri G, Del Nobile MA, Apicella A, Nicolais L (1995) Moisture-matrix interactions in polymer based composite materials. Revue de l'Institut Français du Pétrole 50:551–571
21. Doghieri F, Sarti GC (1996) Nonequilibrium lattice fluids: a predictive model for the solubility in glassy polymers. Macromolecules 29:7885–7896
22. Sarti GC, Doghieri F (1998) Predictions of the solubility of gases in glassy polymers based on the NELF model. Chem Eng Sci 19:3435–3447
23. Scherillo G, Galizia M, Musto P, Mensitieri G (2012) Water sorption thermodynamics in glassy and rubbery polymers: modeling the interactional issues emerging from FTIR spectroscopy. Ind Eng Chem Res. doi:10.1021/ie302350w
24. Giacinti Baschetti M, Doghieri F, Sarti GC (2001) Solubility in glassy polymers: correlations through the nonequilibrium lattice fluid model. Ind Eng Chem Res 40:3027–3037
25. Gibbs JH, Di Marzio EA (1958) Nature of the glass transition and the glassy state. J Chem Phys 28:373–383
26. Gibbs JH (1956) Nature of the glass transition in polymers. J Chem Phys 25:185–186
27. Gibbs JH, Di Marzio EA (1958) Chain stiffness and the lattice theory of polymer phases. J Chem Phys 28:807–813
28. Chow TS (1980) Molecular interpretation of the glass transition temperature of polymer-diluent systems. Macromolecules 13:362–364
29. Gordon JM, Rouse GB, Gibbs JH, Risen WM (1977) The composition dependence of glass transition properties. J Chem Phys 66:4971–4976
30. Ellis TS, Karasz FE (1984) Interaction of epoxy resins with water: the depression of glass transition temperature. Polymer 25:664–669
31. Ellis TS, Karasz FE, ten Brinke G (1983) The influence of thermal properties on the glass transition temperature in styrene/divinylbenzene network-diluent systems. J Appl Polym Sci 28:23–32
32. ten Brinke G, Karasz FE, Ellis TS (1983) Depression of glass transition temperatures of polymer networks by diluents. Macromolecules 16:244–249
33. Panayiotou C, Pantoula M (2006) Sorption and swelling in glassy polymer/carbon dioxide systems: Part I. Sorption. J Supercr Fluids 37:254–262
34. Tsivintzelis I, Angelopoulou AG, Panayiotou C (2007) Foaming of polymers with supercritical CO_2: an experimental and theoretical study. Polymer 48:5928–5939
35. Mensitieri G, Scherillo G (2012) Environmental resistance of high performance polymeric matrices and composites. In: Nicolais L, Borzacchiello A (eds) Wiley encyclopedia of composites, vol. 2, 2nd edn. Wiley, Inc. Hoboken
36. Prinos J, Panayiotou C (1995) Glass transition temperature in hydrogen-bonded polymer mixtures. Polymer 36:1223–1227
37. Kelley FN, Bueche F (1961) Viscosity and glass temperature relations for polymer-diluent systems. J Polym Sci 50:549–556
38. Turnbull D, Cohen M (1959) Molecular transport in liquids and glasses. J Chem Phys 31:1164–1169
39. Turnbull D, Cohen M (1961) Free volume model of the amorphous phase: glass transition. J Chem Phys 34:120–125
40. Marquardt DW (1963) An algorithm for least squares estimation of non linear parameters. J Soc Ind Appl Math 11:431–441
41. Meier RJ (2005) On art and science in curve-fitting vibrational spectra. Vib Spectrosc 39:266–269
42. Noda I, Ozaki Y (2004) Two-dimensional correlation spectroscopy. Wiley, Chichester
43. Noda I, Dowrey AE, Marcott C, Story GM, Ozaki Y (2000) Generalized two-dimensional correlation spectroscopy. Appl Spectrosc 54:236A–248A
44. Ragosta G, Musto P, Abbate M, Scarinzi G (2011) Compatibilizing polyimide/silica hybrids by alkoxisilane-terminated oligoimides: morphology–properties relationships. J Appl Polym Sci 121:2168–2186

45. Musto P, Mensitieri G, Lavorgna M, Scarinzi G, Scherillo G (2012) Combining gravimetric and vibrational spectroscopy measurements to quantify first- and second-shell hydration layers in polyimides with different molecular architectures. J Phys Chem B 116:1209–1220
46. Iwamoto R, Matsuda T (2005) Interaction of water in polymers: poly(ethylene-*co*-vinyl acetate) and poly(vinyl acetate). J Pol Sci: Part B: Pol Phys 43:777–785
47. Tsivintzelis I, Kontogeorgis GM (2009) Modeling the vapor—liquid equilibria of polymer—solvent mixtures: systems with complex hydrogen bonding behavior. Fluid Phase Equilib 280:100–109
48. Fredenslund A, Jones RL, Prausnitz JM (1975) Group-contribution estimation of activity coefficients in nonideal liquid mixtures. AIChE J 21:1086–1099
49. Fredenslund A, Sorensen MJ (1994) Group contribution estimation methods. In: Sandler SI (ed) Models for thermodynamic and phase equilibria calculations. Marcel Dekker, New York
50. Fougnies C, Damman P, Dosière M, Koch MHJ (1997) Time-resolved SAXS, WAXS, and DSC study of melting of poly(aryl ether ether ketone) (PEEK) annealed from the amorphous state. Macromolecules 30:1392–1399
51. Polymer Data Handbook (1999). Mark JE (ed) Oxford University Press, New York
52. Lu SX, Cebe P, Calpel M (1996) Thermal stability and thermal expansion studies of PEEK and related polyimides. Polymer 37:2999–3009
53. Zoller P, Walsh DJ (1995) Standard pressure volume temperature data for polymers. Technomic Publishing AG, Basel
54. Cotugno S, Mensitieri G, Musto P, Sanguigno L (2005) Molecular interactions in and transport properties of densely cross-linked networks: a time-resolved FT-IR spectroscopy investigation of the epoxy/H_2O system. Macromolecules 38:801–811
55. Mensitieri G, Lavorgna M, Musto P, Ragosta G (2006) Water transport in densely crosslinked networks: a comparison between epoxy systems having different interactive character. Polymer 47:8326–8336